

Dislocation-Induced Nanoparticle Decoration on a GaN Nanowire

Bing Yang,^{†,§} Fang Yuan,[†] Qingyun Liu,[†] Nan Huang,[†] Jianhang Qiu,[†] Thorsten Staedler,[‡]
Baodan Liu,^{*,§,†} and Xin Jiang^{*,†,‡,§}

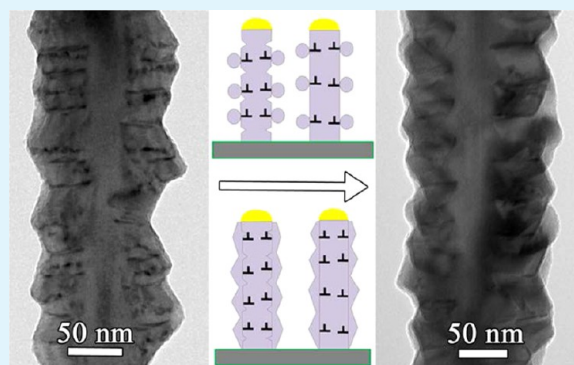
[†]Shenyang National Laboratory for Materials Science, Institute of Metal Research (IMR), Chinese Academy of Sciences (CAS), No. 72 Wenhua Road, Shenyang 110016, China

[‡]Institute of Materials Engineering, University of Siegen, Paul-Bonatz-Str. 9-11, Siegen 57076, Germany

Supporting Information

ABSTRACT: GaN nanowires with homoepitaxial decorated GaN nanoparticles on their surface along the radial direction have been synthesized by means of a chemical vapor deposition method. The growth of GaN nanowires is catalyzed by Au particles via the vapor–liquid–solid (VLS) mechanism. Screw dislocations are generated along the radial direction of the nanowires under slight Zn doping. In contrast to the metal-catalyst-assisted VLS growth, GaN nanoparticles are found to prefer to nucleate and grow at these dislocation sites. High-resolution transmission electron microscopy (HRTEM) analysis demonstrates that the GaN nanoparticles possess two types of epitaxial orientation with respect to the corresponding GaN nanowire: (I) $[\bar{1}2\bar{1}0]_{np} // [\bar{1}2\bar{1}0]_{nw}$, $(0001)_{np} // (0001)_{nw}$; (II) $[\bar{1}2\bar{1}3]_{np} // [\bar{1}2\bar{1}0]_{nw}$, $(10\bar{1}0)_{np} // (10\bar{1}0)_{nw}$. An increased Ga signal in the energy-dispersive spectroscopy (EDS) profile lines of the nanowires suggests GaN nanoparticle growth at the edge surface of the wires. All the crystallographic results confirm the importance of the dislocations with respect to the homoepitaxial growth of the GaN nanoparticles. Here, screw dislocations situated on the (0001) plane provide the self-step source to enable nucleation of the GaN nanoparticles.

KEYWORDS: GaN, nanostructures, dislocation, nucleation, growth



INTRODUCTION

The growth of nanostructures with controlled size and morphology has attracted great research interest in recent years due to the fast development of nanoscale devices.^{1–12} Particular interest has been focused on one-dimensional (1D) nanowires decorated with nanoparticles which offer more opportunities for enhanced properties and application compared with the sole 1D nanowires.^{13–17} Au nanoparticle decorated ZnO nanowires have increased gas sensing response at room temperature compared with pure ZnO nanowires.¹⁸ Pt nanoparticle decorated Si nanowires yield a substantial enhancement in energy conversion efficiency compared with uncovered Si nanowires.¹⁹ It is well accepted that the formation of 1D nanowires with controlled dimensions is generally guided by metal catalyst nanoparticles based on the well-known vapor–liquid–solid (VLS) growth mechanism. During the VLS-based nanowire growth, catalyst nanoparticles in their liquid state serve as nanoscale reactors, by collecting vapor-phase precursor gas and thus forming the eutectics between catalyst and nanostructure materials.^{20,21} The dynamic supersaturation of the catalyst nanoparticles drives the precipitation and growth of a crystalline nanowire. Even more complex nanowire-based architectures such as branched nanowires can be achieved by precisely designing the catalyst structure. For instance, branched GaP nanotrees have been obtained by

controlled seeding of Au catalyst: the growth of the trunk is based on an initial seeding, whereas the branching structure is initiated by a subsequent seeding step.²² Branched InSnO oxide nanowires, on the other hand, are in situ seeded based on a migration of the Au–Cu alloy catalyst, which is responsible for both trunk and branch formation.²¹

Recently, a catalyst-free nanostructure growth driven by screw dislocations has been reported for various semiconductor materials.^{23–26} For example, ZnO nanowires were found to nucleate at the etch pits of dislocations on the surface of a GaN substrate.²⁷ Furthermore, it was observed that the growth of PbS nanopine trees at a low supersaturation was promoted by dislocations that featured a Burgers vector along the nanowire trunk.²³ These dislocations provide self-perpetuating steps at which the branched nanowires form. Essentially, this growth process resembles a catalyst-based VLS growth of nanotree structures. During dislocation-driven nanowire growth, typically a layer by layer growth catalyzed by metal particles is prohibited in the low supersaturation case due to an energy barrier, which hinders the creation of a new surface layer. Growth, however, is possible at dislocation sites as they feature a larger Gibbs

Received: November 14, 2014

Accepted: January 6, 2015

Published: January 6, 2015

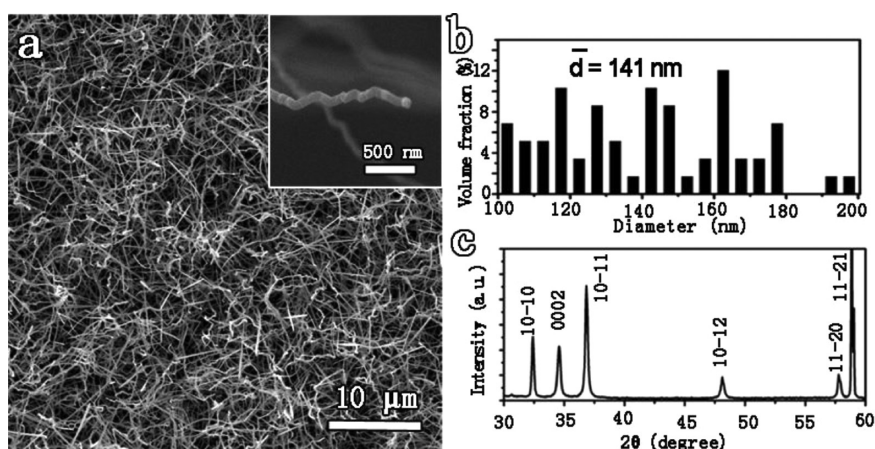


Figure 1. (a) Low-magnification SEM image of the as-synthesized GaN nanowires, in which the inset represents a typical SEM image of the zigzag-shaped GaN nanowire. Statistical diameter distribution (b) and X-ray diffraction pattern (c) collected from the GaN nanowires.

energy. Therefore, catalyst-based growth and the eutectics between the catalyst and nanowire will not be considered for the case of dislocation-driven nucleation of nanostructure. It also implies that the mechanism of dislocation-driven nanowire growth represents a general concept for nanowire formation, which, in principle, can be applied to any material system. A deeper understanding of these mechanisms will eventually lead to defect-based engineering strategies that allow for the synthesis of catalyst-free dislocation-driven nanostructures in the context of specific applications.

In this work, we found that screw dislocations in GaN nanowires facilitated a homogeneous nucleation and growth of GaN nanoparticles along the radial direction of the nanowires. A detailed crystallographic analysis by TEM is able to identify two growth processes that are responsible for the particle nucleation on the GaN nanowires. The first stage is marked by the formation of screw dislocations induced by Zn doping as well as a seeding of the wires with Au catalysts. During the second stage, GaN nanoparticles nucleate and grow along the radial direction of GaN nanowires. This process is driven by the screw dislocation formed in the initial stage.

EXPERIMENTAL SECTION

GaN nanowires decorated by GaN nanoparticles were obtained through a simple chemical vapor deposition (CVD) process as described in our previous work.²⁸ High-purity Ga₂O₃ powders mixed with Zn powders were loaded into an Al₂O₃ crucible as precursors and then inserted into the center of a quartz tube. The Si substrate coated with a thin Au layer (~5 nm) was placed on the downstream area close to the gas outlet for nanowire deposition. The reaction chamber was first cleaned by a flow of Ar gas to remove any residual oxygen and then quickly heated to 900 °C at a constant Ar flow rate of 100 standard cubic centimeters per minute (sccm). Following this step, stable NH₃ gas flowing (100 sccm) replacing the Ar one was introduced to the chamber, and the temperature was increased to 1100 °C for GaN nanowire formation. After reacting at this temperature for 1 h, dark yellow GaN nanostructures were deposited on the surface of the Si substrate. The morphology, the chemical composition, as well as the crystal structure of the products were characterized by X-ray powder diffractometry based on Cu K radiation (XRD, Rigaku D/Max-2400), a scanning electron microscope (SEM, Zeiss supra 55), X-ray photoelectron spectroscopy (XPS, Thermal VG/ESCALAB250), and a high-resolution transmission electron microscope (TEM, FEI Tecnai G2 F20) equipped with a high-angular annular dark-field detector (HAADF) and an X-ray energy-dispersive spectrometer (EDS), respectively.

RESULTS AND DISCUSSIONS

Figure 1a shows a low-magnification SEM image of the as-synthesized GaN nanowires. Obviously, nanowires featuring a straight as well as a zigzag morphology are observed on the Si substrate, which is densely covered by these nanostructures. The high-magnification SEM image shown in the inset of Figure 1a depicts a representative zigzag-shaped GaN nanowire. Statistical investigations on numerous samples reveal a wide range of nanowire diameter in 100–200 nm and a maximum length in the order of several tens of micrometers (Figure 1b). The average diameter of GaN nanowires is about 141 nm. Additionally, Au catalysts are observed at the tip of the GaN nanowire, indicating the VLS growth mode of the nanowires. The XRD pattern shown in Figure 1c reveals that the diffraction peaks centered at $2\theta = 32.4, 34.6, 36.8, 48.1,$ and 57.7° can be well indexed to a standard wurtzite-type GaN with lattice constant of $a = 3.189 \text{ \AA}$ and $c = 5.185 \text{ \AA}$. Comparing this information to the XRD data of pure GaN, no obvious peak shift was found due to the limited Zn doping in the GaN lattice. It is well-known that GaN crystals can exist in either a stable wurtzite (WZ, hexagonal) or a metastable zinc-blende (ZB, cubic) structure.^{29,30} The invasion of impurity dopants into the GaN lattice will lead to a deterioration of the crystallinity of the wires and produce some structural defects such as stacking faults. However, no ZB-GaN phase was observed in the nanowires. The absence of metastable ZB-GaN diffraction peaks in the XRD pattern additionally demonstrates that the as-synthesized GaN nanowires are crystallized in the WZ phase without any Zn-doping-induced phase separation. On the basis of compositional analyses combining EDS with XPS measurements (see Supporting Information, Figures S1 and S2), it appears that the nanowires mainly contain Ga and N in a molar ratio close to 1:1. Though the signal of the Zn dopant was not detected within the EDS resolution limit, the XPS result gives clear evidence for verifying the existence of the Zn dopant in the GaN lattice, as shown in Figure S2d (Supporting Information). Therefore, it can be concluded that the as-synthesized nanowires are actually Zn-doped WZ-GaN phase.

Even though the low solubility of the Zn dopant does not induce any phase transition, it results in a morphological evolution of the nanowires. Furthermore, the introduction of a dopant to a host lattice might induce dislocations in the structure of the GaN nanowires. Figure 2a shows a representative bright-field (BF) TEM image of a GaN nanowire

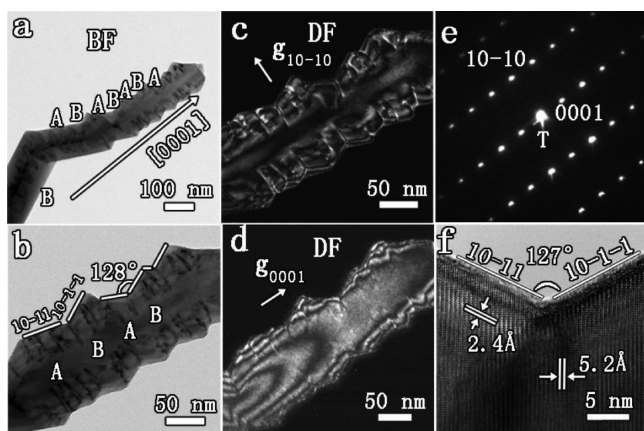


Figure 2. (a) Low-magnification BF TEM image of a zigzag GaN nanowire. (b) High-magnification TEM image showing dislocation within a GaN nanowire. DF image under strong two-beam conditions showing dislocations visible with a diffraction spot of g_{10-10} (c) and invisible with a diffraction spot of g_{0001} (d). SAED pattern (e) and HRTEM image (f) taken along the $[1\bar{2}10]$ zone axis of the nanowire.

that features an irregular corrugated shape. Additionally some short dark-contrast lines perpendicular to the growth direction can clearly be observed. These lines correspond to dislocations formed within the GaN nanowires. It can be seen that the irregular corrugated nanowire consists of alternating segments A and B, which possess different lengths, in Figure 2b. The surface edges of these segments are always parallel with respect to each other displaying an angle between both segments of about 128° . Further analyses on the edge planes by means of selected area electron diffraction (SAED) and HRTEM verified that these periodic planes could be indexed as $(10\bar{1}1)$ and $(10\bar{1}\bar{1})$ planes of the WZ-GaN, respectively. Consequently, the growth axes of segments A and B are the two equivalent crystallographic directions of $[01\bar{1}2]$ and $[01\bar{1}\bar{2}]$, respectively, while the preferential growth plane is (0001) . These segments, that feature different lengths, are responsible for the deviation of growth direction from the standard c axis of the hexagonal WZ-GaN morphology.

In order to judge the crystalline quality and structural defects of the as-synthesized GaN nanowires, SAED, dark-field (DF) imaging, and HRTEM analysis are employed. SAED patterns as well as HRTEM images have been taken along the direction of the zone axis $[1\bar{2}10]$. The observation of sharp and succinct diffraction spots without the presence of an amorphous ring confirms that GaN nanowires are crystallized in the wurtzite phase (Figure 2e), in good agreement with the XRD result (Figure 1b). Furthermore, one can see that the dislocation possesses a certain distribution within the wires in Figure 2b. The highest density of dislocations is observed in the vicinity of the wire surface, whereas the core region of the wire is essentially dislocation free. This distribution was confirmed by studying several tens of GaN nanowires. In this context, the corresponding Burgers vector \vec{b} of the dislocations was determined by evaluation of the diffraction contrast under two beam dark-field conditions (Figure 2c and 2d).³¹ The DF image taken from the $(10\bar{1}0)$ diffraction spot shows high dislocation contrast, while dislocations under the (0001) diffraction spot meet the invisibility criterion with residual contrast, which means that g_{0001} is perpendicular to \vec{b} . As it is also known that the Burgers vector of most dislocations in the hexagonal structure is associated with the $\langle 11\bar{2}0 \rangle$ and $\langle 0001 \rangle$

directions, a fact that has been confirmed in the case of GaN films,^{32,33} it can be concluded that the Burgers vector of the dislocations considered here is along the $\langle 11\bar{2}0 \rangle$ direction. The fact that the Burgers vector is parallel to the dislocation line implies that these dislocations correspond to screw dislocations. Dislocations featuring a Burgers vector of $\langle 11\bar{2}0 \rangle$ are always called “a” dislocations. Considering the residual contrast under (0001) diffraction condition, these “a” dislocations represent mixed dislocations with a predominant screw component. The well-pronounced lattice fringe observed in the HRTEM image shown in Figure 2f further supports the single-crystalline nature of the GaN nanowires. Additionally, it shows the good crystalline quality of the wires. The interspacing of lattice fringes measured by the HRTEM image is 5.2 \AA , which matches well with the (0001) plane interspacing of a standard wurtzite hexagonal GaN structure. The lattice spacing parallel to surface is 2.4 \AA , in good agreement with the d -spacing of the $\{10\bar{1}1\}$ lattice plane of WZ-GaN. However, the core of the screw dislocations is invisible when the dislocation line is perpendicular to the electron beam direction under atomic-resolution imaging conditions. Typically, the formation of dislocation in nanowires can be affected by several factors: first, dislocations can be introduced by substrate effect. For GaN film which has been epitaxially grown on the Al_2O_3 substrate, dislocations initially formed in the substrate were always able to penetrate into the film, forming threading dislocations in the GaN film.³⁴ Threading dislocations, however, are generally observed to lie along the growth direction of as-grown films or nanostructures.^{35,36} In the present work, dislocations are distributed along the radial direction of the GaN nanowires. Consequently, the dislocation nucleation is not directly related to the substrate. Second, dislocations can be induced by mechanical strain during TEM sample preparation, e.g., the transfer of samples from their substrate and ultrasonic treatment process. This possibility can be excluded as no dislocations were identified in dopant-free GaN nanowires even though the same TEM preparation method was applied. Therefore, the growth condition such as temperature and impurity dopant is viewed as the main factor. Especially, the doping of Zn atoms results in local strain and dislocation generation in the GaN nanowire even though the absolute Zn content is below the EDS resolution limit.

Dislocations that feature a core in atomic misalignment possess high Gibbs energy and thus are potentially able to provide a preferential nucleation site for the segregation of other atoms. Figure 3 shows a typical high-magnification SEM image of an as-grown GaN nanowire. One can clearly see that the GaN nanowire has a rough surface morphology featuring many protruding dots, as indicated by white arrows. Figure 4a displays the corresponding TEM image of a zigzag-shaped GaN nanowire that features dislocations at its surface. Some protruding nanoparticles connecting with the dislocations can be observed to grow on the surface of the GaN nanowire, as indicated by the white arrows. Careful TEM examination confirms that these nanoparticles are WZ-GaN in microstructure and composition. This finding implies that GaN nanoparticles prefer to nucleate at these regions where dislocations are located. A HRTEM image taken along the $[1\bar{2}10]$ zone axis (see Figure 4b) reveals that the GaN nanoparticle epitaxially nucleates at the $(10\bar{1}1)$ surface plane of the GaN nanowire. Its orientation relationship can be described as $[1\bar{2}10]_{\text{np}} // [1\bar{2}10]_{\text{nw}}$, $(0001)_{\text{np}} // (0001)_{\text{nw}}$, where the indices np and nw represent the GaN nanoparticle and the GaN

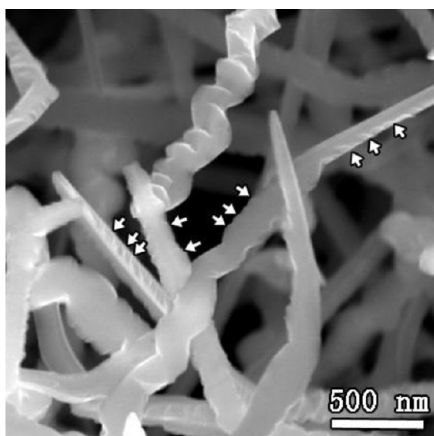


Figure 3. High-magnification SEM image of GaN nanowires that feature a rough-surface morphology.

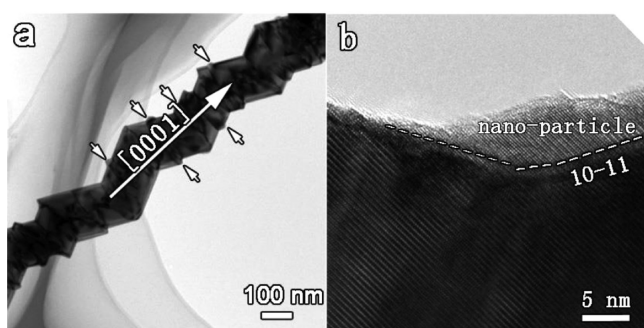


Figure 4. (a) Low-magnification TEM image of a GaN nanowire showing the nucleation of nanoparticles at the surface at positions correlated with the presence of dislocations, indicated by the white arrows. (b) HRTEM image taken along $[1\bar{2}10]$ showing homogeneous epitaxial growth of a GaN nanoparticle along the radial direction of a GaN nanowire.

nanowire, respectively. It has been reported that one-dimensional nanowires can be synthesized on nonplanar substrates based on the so-called terrace ledge kink model.^{37,38} Here, atomic terraces that feature a high surface energy potentially promote a preferential nucleation and sequential guide of the nanowire growth. However, we found the GaN nanoparticles to nucleate far away from any edge-like surface feature of the zigzag nanowire at the flat $(10\bar{1}1)$ plane (Figure 4a). Therefore, the convex surface structure of the zigzag nanowire which potentially features a high surface energy is likely not the key factor to facilitate the nucleation of GaN nanoparticles. Actually, dislocations might play a more important role in this context. The doping of Zn atoms induces local lattice distortion in the GaN lattice. Segregation of doped atoms could lead to larger strain and the formation of dislocations, which favors the nucleation of GaN nanoparticles due to the high Gibbs energy.^{24,39,40}

Figure 5a shows a low-magnification TEM image of a typical straight nanowire that features a rough surface. Again, the dislocation distribution resembles the one observed in the case of the zigzag nanowire (see Figure 2). The high-magnification BF as well as its corresponding DF image reveals that many GaN nanoparticles are nucleated at dislocation sites along the radial direction of the GaN nanowire, as marked by the arrows in Figure 5b and 5c. These nanoparticles overlap with the side region of GaN nanowires, while no nanoparticles nucleate in

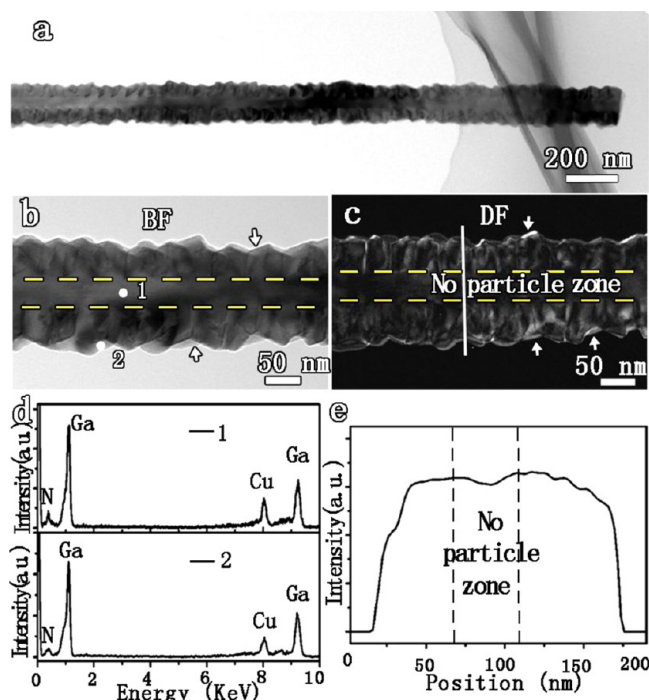


Figure 5. (a) Low-magnification image of a GaN nanowire featuring a rough-surface morphology that indicates the growth of a nanoparticle. BF image (b) and DF image (c) showing the overlap between GaN nanoparticles and the nanowire at the upper and lower surface of the nanowire. (d) EDS spectra taken at the regions labeled “1” and “2” in (b), respectively. (e) EDS intensity profile along the radial direction.

the middle region of the nanowire. Such GaN nanowires are easily confused with the GaN nanotube due to the characteristic contrast differences. To study any chemical composition difference within such a GaN nanowire, EDS measurements using a small electron beam size were carried out in two modes, a point mode and a line-scan mode. The point mode was applied at two representative areas, a center part (“1”) and the nanoparticle edge (“2”), respectively. The line scan mode was used to sample an elemental profile along the radial direction of the wire. Figure 5d shows the corresponding EDS spectra of the two areas “1” and “2”. It can be noted that only N and Ga signals are detected at these two areas, verifying that such a structure is composed of a rough GaN nanowire that is decorated with GaN nanoparticles. The Cu peaks in the EDS spectra come from the TEM Cu grid utilized in this study. The EDS line-scan profile of the Ga element along the radial direction of the GaN nanowire shows pronounced signals at the edge of the nanowire. This suggests an increased material depth at the overlap region compared to the central region of the wire (Figure 5e). The intensive Ga peak signals at the edge further confirm that GaN nanoparticles are decorated at the edge of the GaN nanowire. Therefore, it can be concluded again that GaN nanoparticles are preferentially nucleated at the dislocation region of the GaN nanowire, and this assertion was further evidenced by the fact that no GaN nanoparticles could be found at the region free of dislocations. Here, the central concave region between the dashed lines, showing a width of 50 nm, corresponds to the solid core of the nanowire which features no GaN nanoparticle decoration.

Figure 6a shows a HRTEM image of a GaN nanowire that features a decoration with GaN nanoparticles taken along the $[1\bar{2}10]$ zone axis. The nanowire itself grows along the $[0001]$

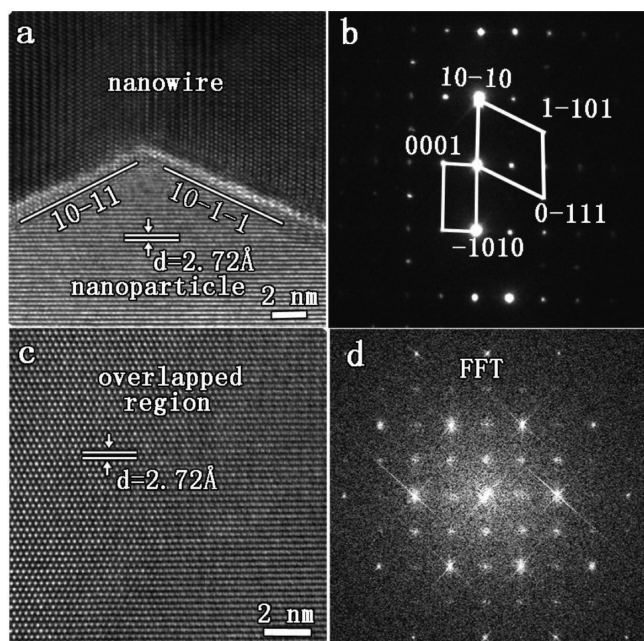


Figure 6. (a) HRTEM image of the homogeneous epitaxial growth of a GaN nanoparticle along the radial direction of a GaN nanowire taken along the $[1\bar{2}10]$ zone axis of the nanowire. (b) The corresponding SAED pattern of the nanostructure. (c) HRTEM image of the overlapped region between the GaN particle and nanowire. (d) The corresponding FFT of (c) showing two oriented phases.

direction. Additionally, it can be observed that the $(10\bar{1}0)$ plane of the GaN nanoparticles is aligned parallel to the same plane of the nanowire. This is a clear indication for an epitaxial nucleation and growth of the particles on the wire surface. Figure 6b represents the corresponding SAED pattern taken at the overlapping region of the GaN nanoparticle and GaN nanowire. Their orientation relationship is determined to be as follows: $[1\bar{2}\bar{1}3]_{np} // [1\bar{2}\bar{1}0]_{nw}$, $(10\bar{1}0)_{np} // (10\bar{1}0)_{nw}$, which is different from the relationship found in Figure 4. Figure 6c shows the corresponding HRTEM image taken at the overlap region along the $[1\bar{2}\bar{1}3]$ zone axis of the WZ-GaN structure. The interspacing of the lattice fringe measured from the HRTEM image is 2.7 Å, which matches well with the lattice spacing of the $(10\bar{1}0)$ plane of hexagonal GaN. Moiré fringes resulting from the overlap between the GaN particle and the GaN nanowire can also be observed, as shown in the right part of Figure 6c. The corresponding FFT pattern of the HRTEM image (Figure 6d) shows two sets of succinct spots, demonstrating again the epitaxial nucleation of GaN nanoparticles on GaN nanowires as they share their $(10\bar{1}0)$ plane. In contrast to the low nucleation density of GaN nanoparticles on GaN nanowires, occasionally a continuous decoration of the GaN nanowire by GaN nanoparticles is observed. In such a case the nanoparticles form a complete shell covering the nanowire. Figure 7 shows the BF and the corresponding DF image of coalesced GaN nanoparticles on the surface. It was noted that GaN nanoparticles prefer to initially nucleate at the surface of the nanowire that contains dislocations in a homogeneous fashion and subsequently evolve into a continuous shell. To illustrate the dislocation-driven formation process of GaN nanoparticles on GaN nanowires, a growth model is proposed in Figure 8. First, GaN nanowires are seeded by a Au catalyst via the VLS mechanism. At the same time, dislocations along the radial direction of GaN nanowires will be induced by a

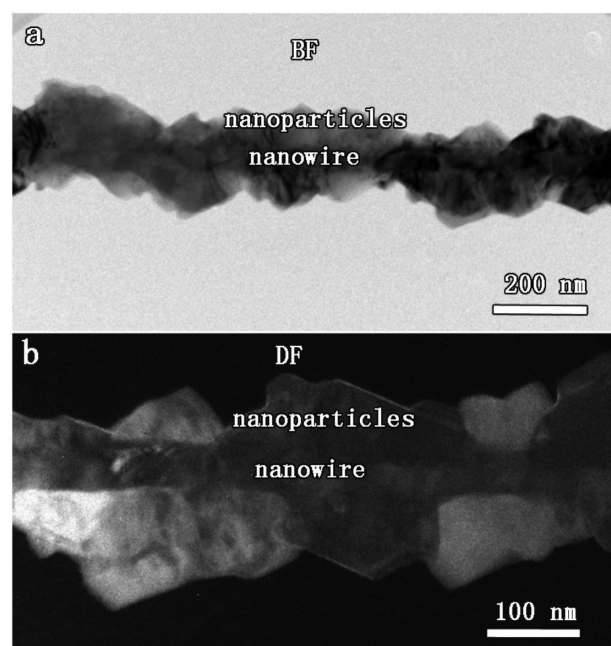


Figure 7. TEM BF image (a) and DF image (b) showing large GaN particles enclosing a GaN nanowire.

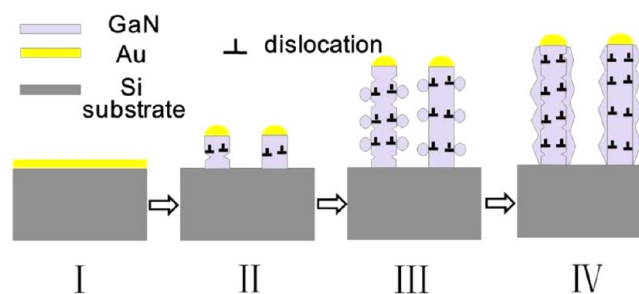


Figure 8. Schematic illustration of the growth of GaN nanowires decorated with nanoparticles driven by dislocations.

slight Zn doping. In the second stage, the dislocations provide the appropriate sites for a homoepitaxial nucleation of GaN nanoparticles on the wires. Finally the GaN nanoparticles coalesce.

It is well-known that the impurity doping affects the growth behavior or thermodynamics of nanostructures and will typically cause significant changes of morphology and geometrical shape.⁴¹ A previous work dedicated to P-doped GaN nanowires verified that the morphology of GaN nanowires evolved from a smooth to a rough surface after doping.⁴² Additionally, it has been reported that Zn doping at a level of about 10^{21} cm^{-3} is able to induce a morphology transformation from a GaN nanowire to a nanotube.⁴³ The surface morphology and geometrical shape of GaN nanowires appear to be quite sensitive to the addition of foreign impurities. It is likely that the dislocation density and nanoparticle nucleation density will be significantly enhanced by an increase of the doping concentration. In such a case the surface of the GaN nanowires will become extremely rough due to homogeneous decoration of GaN nanoparticles. The core of a dislocation is able to accelerate the atomic diffusion at high temperatures like a pipe.⁴⁴ During the synthesis process, the atoms in the GaN nanowire core could migrate to the surface via such dislocation pipes and consequently form hollow GaN nanotubes. The role

of dislocation is providing an explanation for the observation of a formation of the GaN nanotube which is induced by Zn doping of GaN nanowires.⁴³ The dislocation-driven homogeneous decoration of the GaN nanowire offers a path to realize a novel nanoarchitecture as well as the potential to tailor the optoelectronic properties of GaN nanowires. For instance, three-dimensional GaN nanotrees required for specific applications can potentially be obtained by controlling the local doping concentration and, in turn, the dislocation sites. The approach proposed in this work can be applied to the synthesis of a wide range of semiconductor nanostructures and will potentially lead to new structures that feature improved properties.

CONCLUSION

In summary, we report a dislocation-driven formation of GaN nanoparticles on GaN nanowires induced by a slight Zn doping. It was observed that the dislocations were preferentially generated at the edge of the GaN nanowire structure. The weak-beam dark-field image confirms these dislocations feature a predominant screw Burgers component of $\langle 11\bar{2}0 \rangle$. The central region of the nanowire essentially stayed dislocation free. GaN nanoparticles preferred to nucleate on the dislocation sites in an epitaxial manner. Two types of orientation relationship were identified for the nanoparticle growth on the GaN nanowires: (I) $[\bar{1}2\bar{1}0]_{np} // [\bar{1}2\bar{1}0]_{nw}$, $(0001)_{np} // (0001)_{nw}$; (II) $[\bar{1}2\bar{1}3]_{np} // [\bar{1}2\bar{1}0]_{nw}$, $(10\bar{1}0)_{np} // (10\bar{1}0)_{nw}$. An increased concentration of Ga at the edges of the GaN nanowire, which was confirmed by EDS profiles, indicates these edges as preferential nucleation sites of the GaN nanoparticles. The results elucidated that dislocations are responsible for the decoration of GaN nanowires with the corresponding nanoparticles. It is assumed that this finding represents a general design path for the synthesis of various complex three-dimensional semiconductor nanostructures that will potentially feature attractive optoelectronic properties.

ASSOCIATED CONTENT

Supporting Information

EDS and XPS spectra collected from the as-synthesized GaN nanowires. This material is available free of charge via the Internet at <http://pubs.acs.org>.

AUTHOR INFORMATION

Corresponding Authors

*E-mail: baodanliu@imr.ac.cn.

*E-mail: xjiang@imr.ac.cn.

Author Contributions

[§]These authors contributed equally.

Notes

The authors declare no competing financial interest.

ACKNOWLEDGMENTS

B. Yang and B. D. Liu would like to thank the National Nature Science Foundation of China (Grants No. 51402309 and 51102034) and the Knowledge Innovation Program of Institute of Metal Research (IMR), Chinese Academy of Science (CAS) (grants No. Y2NCA111A1 and Y3NCA111A1) and the Youth Innovation Promotion Association, Chinese Academy of Sciences (Grant No. Y4NC711171) for the support of this work.

REFERENCES

- (1) Algra, R. E.; Verheijen, M. A.; Borgstrom, M. T.; Feiner, L. F.; Immink, G.; van Enckevort, W. J. P.; Vlieg, E.; Bakkers, E. Twinning Superlattices in Indium Phosphide Nanowires. *Nature* **2008**, *456*, 369–372.
- (2) Lao, J. Y.; Wen, J. G.; Ren, Z. F. Hierarchical ZnO Nanostructures. *Nano Lett.* **2002**, *2*, 1287–1291.
- (3) Shin, N.; Chi, M.; Howe, J. Y.; Filler, M. A. Rational Defect Introduction in Silicon Nanowires. *Nano Lett.* **2013**, *13*, 1928–1933.
- (4) Tsvion, D.; Schwartzman, M.; Popovitz-Biro, R.; von Huth, P.; Joselevich, E. Guided Growth of Millimeter-long Horizontal Nanowires with Controlled Orientations. *Science* **2011**, *333*, 1003–1007.
- (5) Hillerich, K.; Dick, K. A.; Wen, C. Y.; Reuter, M. C.; Kodambaka, S.; Ross, F. M. Strategies to Control Morphology in Hybrid Group III-V/Group IV Heterostructure Nanowires. *Nano Lett.* **2013**, *13*, 903–908.
- (6) Sahoo, P.; Dhara, S.; Amirthapandian, S.; Kamruddin, M. Evolution of GaN Nanowire Morphology during Catalyst-induced Growth Process. *J. Mater. Chem. C* **2013**, *1*, 7237–7245.
- (7) Beaudry, A. L.; LaForge, J. M.; Tucker, R. T.; Sorge, J. B.; Adamski, N. L.; Li, P.; Taschuk, M. T.; Brett, M. J. Directed Branch Growth in Aligned Nanowire Arrays. *Nano Lett.* **2014**, *14*, 1797–1803.
- (8) Liu, B. D.; Yuan, F.; Dierre, B.; Sekiguchi, T.; Zhang, S.; Xu, Y. K.; Jiang, X. Origin of Yellow-band Emission in Epitaxially Grown GaN Nanowire Arrays. *ACS Appl. Mater. Interfaces* **2014**, *6*, 14159–14166.
- (9) Bie, Y. Q.; Liao, Z. M.; Wang, P. W.; Zhou, Y. B.; Han, X. B.; Ye, Y.; Zhao, Q.; Wu, X. S.; Dai, L.; Xu, J.; Sang, L. W.; Deng, J. J.; Laurent, K.; Leprince-Wang, Y.; Yu, D. P. Single ZnO Nanowire/p-type GaN Heterojunctions for Photovoltaic Devices and UV Light-emitting Diodes. *Adv. Mater.* **2010**, *22*, 4284–4287.
- (10) Hong, Y. J.; Lee, C. H.; Beom Park, J.; Jin An, S.; Yi, G. C. GaN Nanowire/thin Film Vertical Structure p–n Junction Light-emitting Diodes. *Appl. Phys. Lett.* **2013**, *103*, 261116–1–5.
- (11) Kibria, M. G.; Nguyen, H. P. T.; Cui, K.; Zhao, S. R.; Liu, D. P.; Guo, H.; Trudeau, M. L.; Paradis, S.; Hakima, A. R.; Mi, Z. T. One-Step Overall Water Splitting under Visible Light Using Multiband InGaN/GaN Nanowire Heterostructures. *ACS Nano* **2013**, *7*, 7886–7893.
- (12) Howell, S. L.; Padalkar, S.; Yoon, K.; Li, Q. M.; Koleske, D. D.; Wierer, J. J.; Wang, G. T.; Lauhon, L. J. Spatial Mapping of Efficiency of GaN/InGaN Nanowire Array Solar Cells Using Scanning Photocurrent Microscopy. *Nano Lett.* **2013**, *13*, 5123–5128.
- (13) Galopin, E.; Barbillat, J.; Coffinier, Y.; Szunerits, S.; Patriarche, G.; Boukherroub, R. Silicon Nanowires Coated with Silver Nanostructures as Ultrasensitive Interfaces for Surface-Enhanced Raman Spectroscopy. *ACS Appl. Mater. Interfaces* **2009**, *1*, 1396–1403.
- (14) Berven, C. A.; Dobrokhotov, V.; McIlroy, D. N.; Chava, S.; Abdelrahman, R.; Heieren, A.; Dick, J.; Barredo, W. Gas Sensing With Mats of Gold-Nanoparticle Decorated GaN Nanowires. *IEEE Sens. J.* **2008**, *8*, 930–935.
- (15) Claessens, N.; Demoisson, F.; Dufour, T.; Mansour, A.; Felten, A.; Guillot, J.; Pireaux, J. J.; Reniers, F. Carbon Nanotubes Decorated with Gold, Platinum and Rhodium Clusters by Injection of Colloidal Solutions into the Post-discharge of an RF atmospheric Plasma. *Nanotechnology* **2010**, *21*, 385603.
- (16) Ruffino, F.; Grimaldi, M. G. Au Nanoparticles Decorated SiO₂ Nanowires by Dewetting on Curved Surfaces: Facile Synthesis and Nanoparticles–nanowires Sizes Correlation. *J. Nanopart. Res.* **2013**, *15*, 1–17.
- (17) Assmus, T.; Balasubramanian, K.; Burghard, M.; Kern, K.; Scolari, M.; Fu, N.; Myalitsin, A.; Mews, A. Raman Properties of Gold Nanoparticle-decorated Individual Carbon Nanotubes. *Appl. Phys. Lett.* **2007**, *90*, 17109–1–3.
- (18) Joshi, R. K.; Hu, Q.; Am, F.; Joshi, N.; Kumar, A. Au Decorated Zinc Oxide Nanowires for CO Sensing. *J. Phys. Chem. C* **2009**, *113*, 16199–16202.

- (19) Peng, K. Q.; Wang, X.; Wu, X. L.; Lee, S. T. Platinum Nanoparticle Decorated Silicon Nanowires for Efficient Solar Energy Conversion. *Nano Lett.* **2009**, *9*, 3704–3709.
- (20) Xia, Y. N.; Yang, P. D.; Sun, Y. G.; Wu, Y. Y.; Mayers, B.; Gates, B.; Yin, Y. D.; Kim, F.; Yan, Y. Q. One-dimensional Nanostructures: Synthesis, Characterization, and Applications. *Adv. Mater.* **2003**, *15*, 353–389.
- (21) Gao, J.; Lebedev, O. I.; Turner, S.; Li, Y. F.; Lu, Y. H.; Feng, Y. P.; Boullay, P.; Prellier, W.; van Tendeloo, G.; Wu, T. Phase Selection Enabled Formation of Abrupt Axial Heterojunctions in Branched Oxide Nanowires. *Nano Lett.* **2012**, *12*, 275–280.
- (22) Dick, K. A.; Deppert, K.; Larsson, M. W.; Martensson, T.; Seifert, W.; Wallenberg, L. R.; Samuelson, L. Synthesis of Branched 'Nanotrees' by Controlled Seeding of Multiple Branching Events. *Nat. Mater.* **2004**, *3*, 380–384.
- (23) Bierman, M. J.; Lau, Y. K. A.; Kvit, A. V.; Schmitt, A. L.; Jin, S. Dislocation-driven Nanowire Growth and Eshelby Twist. *Science* **2008**, *320*, 1060–1063.
- (24) Zhuang, A.; Li, J. J.; Wang, Y. C.; Wen, X.; Lin, Y.; Xiang, B.; Wang, X. P.; Zeng, J. Screw Dislocation Driven Bidirectional Spiral Growth of Bi₂Se₃ Nanoplates. *Angew. Chem., Int. Ed.* **2014**, *53*, 6425–6429.
- (25) Meng, F.; Morin, S. A.; Forticaux, A.; Jin, S. Screw Dislocation Driven Growth of Nanomaterials. *Acc. Chem. Res.* **2013**, *46*, 1616–1626.
- (26) Wu, H. Y.; Meng, F.; Li, L. S.; Jin, S.; Zheng, G. F. Dislocation-driven CdS and CdSe Nanowire Growth. *ACS Nano* **2012**, *6*, 4461–4468.
- (27) Morin, S. A.; Jin, S. Screw Dislocation-driven Epitaxial Solution Growth of ZnO Nanowires Seeded by Dislocations in GaN Substrates. *Nano Lett.* **2010**, *10*, 3459–3463.
- (28) Yuan, F.; Liu, B.; Wang, Z.; Yang, B.; Yin, Y.; Dierre, B.; Sekiguchi, T.; Zhang, G.; Jiang, X. Synthesis, Microstructure, and Cathodoluminescence of 0001 -Oriented GaN Nanorods Grown on Conductive Graphite Substrate. *ACS Appl. Mater. Interfaces* **2013**, *5*, 12066–12072.
- (29) Zhou, X. T.; Sham, T. K.; Shan, Y. Y.; Duan, X. F.; Lee, S. T.; Rosenberg, R. A. One-dimensional Zigzag Gallium Nitride Nanostructures. *J. Appl. Phys.* **2005**, *97*, 104315–1–6.
- (30) Jacobs, B. W.; Ayres, V. M.; Petkov, M. P.; Halpern, J. B.; He, M. Q.; Baczewski, A. D.; McElroy, K.; Crimp, M. A.; Zhang, J. M.; Shaw, H. C. Electronic and Structural Characteristics of Zinc-blende Wurtzite Biphasic Homostructure GaN Nanowires. *Nano Lett.* **2007**, *7*, 1435–1438.
- (31) Williams, D. B.; Carter, C. B. *Transmission Electron Microscopy: a Textbook for Materials science*, 1st ed.; Plenum Press: New York, 1996.
- (32) Romano, L. T.; Krusor, B. S.; Molnar, R. J. Structure of GaN Films Grown by Hydride Vapor Phase Epitaxy. *Appl. Phys. Lett.* **1997**, *71*, 2283–2285.
- (33) Vennegues, P.; Beaumont, B.; Vaille, M.; Gibart, P. Microstructure of GaN Epitaxial Films at Different Stages of the Growth Process on Sapphire (0001). *J. Cryst. Growth* **1997**, *173*, 249–259.
- (34) Kappers, M. J.; Datta, R.; Oliver, R. A.; Rayment, F. D. G.; Vickers, M. E.; Humphreys, C. J. Threading Dislocation Reduction in (0001) GaN Thin Films Using SiN_x Interlayers. *J. Cryst. Growth* **2007**, *300*, 70–74.
- (35) Moram, M. A.; Ghedia, C. S.; Rao, D. V. S.; Barnard, J. S.; Zhang, Y.; Kappers, M. J.; Humphreys, C. J. On the Origin of Threading Dislocations in GaN Films. *J. Appl. Phys.* **2009**, *106*, 073513–1–9.
- (36) Wang, Y. Q.; Liang, W. S.; Petrov, P. K.; Alford, N. M. Dissociation of Misfit and Threading Dislocations in Ba_{0.75}Sr_{0.25}TiO₃ Epitaxial Film. *Mater. Charact.* **2011**, *62*, 294–297.
- (37) Zhang, Z. Y.; Lagally, M. G. Atomistic processes in the Early Stages of Thin-film Growth. *Science* **1997**, *276*, 377–383.
- (38) Zou, Q.; Liu, M.; Wang, G. Q.; Lu, H. L.; Yang, T. Z.; Guo, H. M.; Ma, C. R.; Xu, X.; Zhang, M. H.; Jiang, J. C.; Meletis, E. I.; Lin, Y.; Gao, H. J.; Chen, C. L. Step Terrace Tuned Anisotropic Transport Properties of Highly Epitaxial LaBaCo₂O_{5.5+δ} Thin Films on Vicinal SrTiO₃ Substrates. *ACS Appl. Mater. Interfaces* **2014**, *6*, 6704–6708.
- (39) Duguay, S.; Philippe, T.; Cristiano, F.; Blavette, D. Direct Imaging of Boron Segregation to Extended Defects in Silicon. *Appl. Phys. Lett.* **2010**, *97*, 242104–1–3.
- (40) Bellmann, M. P.; Kaden, T.; Kressner-Kiel, D.; Friedl, J.; Möller, H. J.; Arnberg, L. The Impact of Germanium Doping on the Dislocation Distribution in Directional Solidified mc-Silicon. *J. Cryst. Growth* **2011**, *325*, 1–4.
- (41) Sieber, B.; Salonen, J.; Makila, E.; Tenho, M.; Heinonen, M.; Huhtinen, H.; Paturi, P.; Kukkk, E.; Perry, G.; Addad, A.; Moreau, M.; Boussekey, L.; Boukherroub, R. Ferromagnetism Induced in ZnO Nanorods by Morphology Changes under a Nitrogen-carbon Atmosphere. *RSC Adv.* **2013**, *3*, 12945–12954.
- (42) Liu, B. D.; Bando, Y.; Tang, C. C.; Xu, F. F.; Golberg, D. Excellent Field-emission Properties of P-doped GaN Nanowires. *J. Phys. Chem. B* **2005**, *109*, 21521–21524.
- (43) Xie, X.; Wang, G. Z.; Shao, Z. B.; Li, D. P. Zn-doped Gallium Nitride Nanotubes with Zigzag Morphology. *J. Phys. Chem. C* **2009**, *113*, 14633–14637.
- (44) Legros, M.; Dehm, G.; Arzt, E.; Balk, T. Observation of Giant Diffusivity along Dislocation Cores. *Science* **2008**, *319*, 1646–1649.